Aeolian Research 74 (2025) 100997

Contents lists available at ScienceDirect

Aeolian Research

journal homepage: www.elsevier.com/locate/aeolia

Full Length Article

Provenance of sediments in a deep-sea core offshore Kangaroo Island spanning the last 125 ka

Jan-Berend W. Stuut [a,b,*], Patrick De Deckker [c], Rick Hennekam [a]

[a] NIOZ – Royal Netherlands Institute for Sea Research, Ocean Systems Dept., Texel, The Netherlands
[b] VU – Vrije Universiteit Amsterdam, Faculty of Science, Earth Sciences Dept., Amsterdam, The Netherlands
[c] ANU – Australian National University, Research School of Earth Sciences, Canberra, Australia

ARTICLE INFO

Keywords:
Provenance
PSA – potential source areas
XRF core scanning
Aeolian dust
Fluvial sediments
Late Quaternary
Murray-Darling Basin
Central and southern South Australia

ABSTRACT

It is common practice nowadays to assess the presence of terrigenous (land-derived) sediments in deep-sea cores using bulk geochemical data, but the key issue is to identify the source of these sediments and the way they were transported to the core site in order to interpret their palaeoclimatic significance. Here, we demonstrate a new approach taken to geochemically-fingerprint a large set of sediments collected from potential source areas (PSAs) in southeastern and southcentral Australia and to compare these data with the record obtained from X-ray Fluorescence (XRF) scanning on a long deep-sea sediment core MD03-2607 obtained offshore Kangaroo Island, South Australia. The entire data set of samples collected on land as well as the downcore measurements were unmixed using the numerical end-member method AnalySize. We successfully use the elements Al, Fe, K, Mn, S, Sr and Y to define end members. In addition, the on-land occurrences of the chemical ratios of Zr/Zn, Ti/Rb, Ti/Y and Zr/Rb are used to support the provenance of the chemical end-members. Three main PSA's are defined: Murray River Basin (MRB), Darling River Basin (DRB) and Kati Thanda – Lake Eyre District (LED), of which the MRB is represented in two different chemical end members. The downcore contributions of these end members in the sediment core are consequently interpreted in terms of fluvial (MRB and DRB) versus aeolian (LED) input. We determined the origin of the terrigenous sediments recovered from the core for the last glacial-interglacial cycle, with implications for atmospheric circulation across southern Australia.

Introduction

Determining sediment provenance from marine cores using bulk geochemical composition is a well-established approach. However, just as the composition of geological provinces is not uniform across the world, there is no standard elemental ratio directly applicable to deep-sea sediments to determine the provenance of the terrigenous sediment fraction delivered at sea. In addition, the sediment-transport mechanisms leading to eventual deposition of terrigenous material at sea may influence its geochemical composition. For example, Lamy et al. (2001) and Haug et al. (2001) present the occurrence of the single element iron (Fe) in deep-sea sediments on the proximal Chilean and Venezuelan continental slopes as a proxy for continental humidity-driven runoff whereas Lamy et al. (2014) use the occurrence of the same element as a proxy for the proportion of aeolian dust in distal deep-sea sediments in the South Pacific Ocean. On the other hand, Stuut et al. (2014; 2019) and McGregor et al. (2009) use the ratio (Fe/Ca) as a proxy for terrigenous-sediment input in deep-sea sediments on the proximal Australian- and northwest African continental slopes, respectively. In much the same way, the ratio (Ti/Ca) was presented as a proxy for terrestrial input into the western Pacific Ocean (Tjallingii et al., 2010) and eastern Indian Ocean (Stuut et al., 2019).

Different studies have applied various elemental ratios, such as Ti/Al and Zr/Rb, as proxies to reconstruct past dust content and particle size in marine sediments, although their effectiveness can be influenced by sediment source mixing and requires detailed knowledge of source sediments for accurate interpretation (Boyle, 1983; Zabel et al., 1999, 2001; Matthewson et al., 1995; Prins et al., 2001; Stuut et al., 2019; Hennekam et al., 2022). Such the unmixing of sediment sources from marine records is typically hampered by the lack of geochemical knowledge of the source areas. Here, we show a unique dataset of southcentral and southeastern Australia for which we acquired detailed geochemical data from both the source region, as well as its downward variation over the last 125 kyr in a single deep-sea core located offshore

* Corresponding author at: NIOZ – Royal Netherlands Institute for Sea Research, Ocean Systems dept., Texel, The Netherlands.
E-mail address: jan-berend.stuut@nioz.nl (J.-B.W. Stuut).

https://doi.org/10.1016/j.aeolia.2025.100997
Received 8 May 2025; Received in revised form 8 July 2025; Accepted 12 August 2025
Available online 20 August 2025

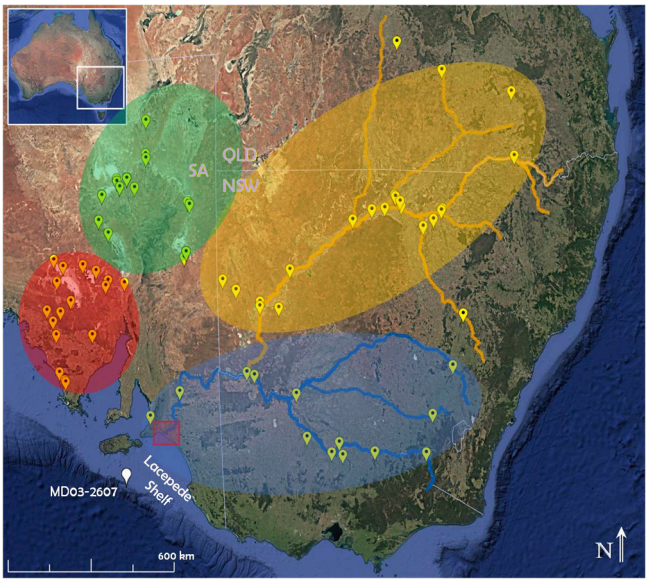

Fig. 1. Map of the study area. Yellow pins: positions of samples collected along the main rivers (Darling River and River Murray) as well as at the edges of dry playas in South Australia (see De Deckker 2019; 2020). White pin: core location. Blue lines: River Murray and tributaries, Orange lines: Darling River and tributaries. The River Murray Mouth is shown by a red square. The states of Queensland (QLD), New South Wales (NSW) and South Australia (SA) are indicated in yellow. Four potential areas are indicated based on the initial grouping of samples using element ratios, shown in (For interpretation of the references to colour in this figure legend, the reader is referred to the web version of this article.)
Source Fig. 3.

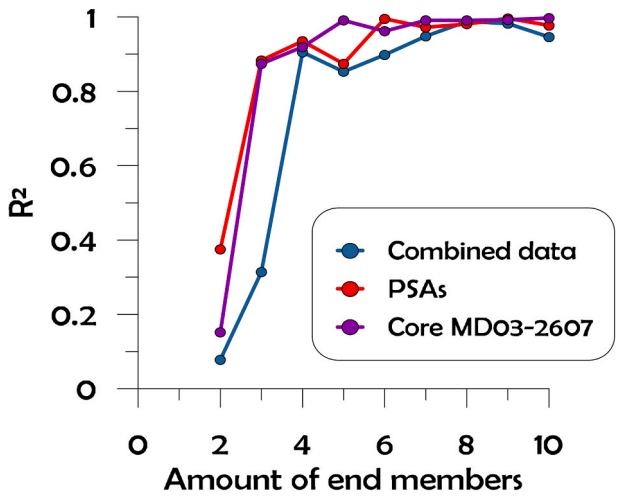

Fig. 2. Goodness −of-fit statistics showing the increasing reproducibility of the data (R^2) with increasing end members. Already with N = 4 end members > 90 % of the variability in the combined data set can be explained.

the exit of the entire Murray Darling Basin. Doing so, allows us to test a new approach using end members to unmix our dataset of bulk chemical composition to reconstruct changes in sediment sources over time for this region, ultimately allowing us to track the major drivers of potential source area (PSA) change over the last glacial to present. We firmly believe that using PSAs are the best way to ascertain the origin of material (via their trace elemental and/or isotopic composition) as source areas such as deflation basins do not change composition over time. This allows the determination of material from source areas to be established over long periods of time, such as a glacial interglacial cycle, and even for longer periods of time.

Here specifically, we present a comparison of the chemical composition of (N = 72) present-day on-land PSAs in central and western South Australia, as well as from confluents of the Murray-Darling Rivers, which we compare with chemical analyses of a sediment core from offshore Kangaroo Island (Fig. 1) that covers the last 125 kyr. There is no need to discuss PSA's from further east in Australia as winds principally go from west to east, and therefore material from those regions could not be transported towards the core site off Kangaroo Island. The core site acts as a depocenter for terrigenous sediments transported both by rivers through a single outlet (River Murray Mouth) and wind from land to sea, coming from either north of the site (such as the Lake Eyre Basin), and the west of South Australia and nearby Murray Darling Basin. This dataset was consequently 'unmixed' into individual end members, which were used to characterise the individual source regions: River Murray Basin (MRB), Darling River Basin (DRB) and Kati Thanda – Lake Eyre District (LED). This way, we could quantify the downcore contributions from these different PSAs throughout the last 125 kyr and interpret their contribution in terms of paleoclimatic changes. This is the first time such an approach has been pursued.

The Murray-Darling Basin

The Murray Darling Basin (MDB) is one of the largest internal-drainage basins of Australia with a single river outlet to the ocean, the mouth of the River Murray (Fig. 1). The basin covers some $1.6x10^6$ km^2 and can be divided geologically into two separate sub-basins, based on their respective geologies: the Murray sub-basin and the Darling sub-basin (refer to Gingele et al. (2004)). The northern tributaries of the Darling River originate from south-central Queensland where Mesozoic clastic sediments outcrop, whereas the eastern tributaries drain the western slopes of the Great Dividing Range which consist of Tertiary mafic volcanics, Mesozoic granites and Late Palaeozoic volcanics, as well as metasediments; these form the southern part of the New England Fold Belt. The River Murray and its tributaries instead drain the Lachlan Foldbelt which consists predominantly of Palaeozoic granites, volcanics and metasediments. Thus, because of the different geological entities, it is possible to distinguish samples from the two sub-basins. Already, Gingele and De Deckker (2004) were able to separate different parts of the MDB based on different clay mineralogies. Similarly, Gingele and De Deckker (2005) also used trace elements and Sr and Nd isotopes to further separate samples from the Murray sub-basin from the Darling sub-basin. This eventually permitted Gingele et al. (2007) to identify the principal source of sediments recovered from core MD03-2607 spanning the last 17 kyr of sedimentation. The geochemical work of these latter authors dealt with the fluvial component of sediments deposited at sea. This study mentioned above was extended by Bayon et al. (2017) who used Nd isotopes obtained from an adjacent core (MD03-2611 some 60 km to the west) to determine the provenance of fluvial sediments from the MDB. This study only covered the last 85 kyr of deposition at sea, following the revised age model by De Deckker et al. (2021).

PSAs of dust in south and western South Australia

De Deckker (2019, 2020) provided ample information of the sites that were identified as airborne dust PSA in central and western South Australia, a region that is located to the north and west of core MD03-2607 and up wind. For further information on wind patterns in this region, refer to the seminal study by Sprigg (1979). This region is geologically very diverse, ranging from Archean to Late Cainozoic lithologies (see De Deckker, 2019: Fig. 21). No rivers drain this region towards the core site and, therefore, any material originating from this area must have been of aeolian (wind-blown) origin.

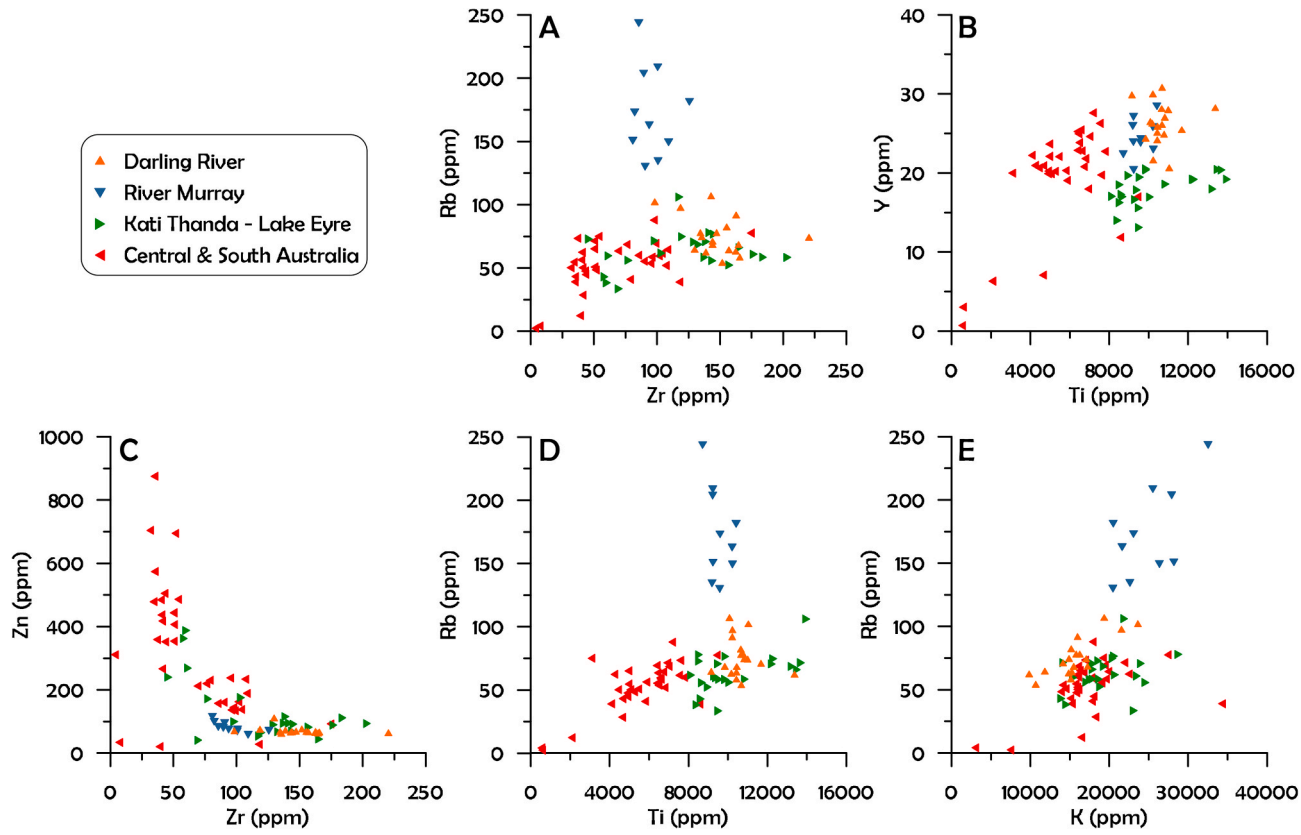

Fig. 3. Characterisation of the PSA samples distributed into four groups: Darling River, River Murray, Kati Thanda – Lake Eyre and central and western South Australia on the basis of selected element ratios **A**: Rb versus Zr and **B**: Y versus Ti, **C**: Zr versus Zn, **D**: Ti versus Rb, and **E**: K versus Rb.

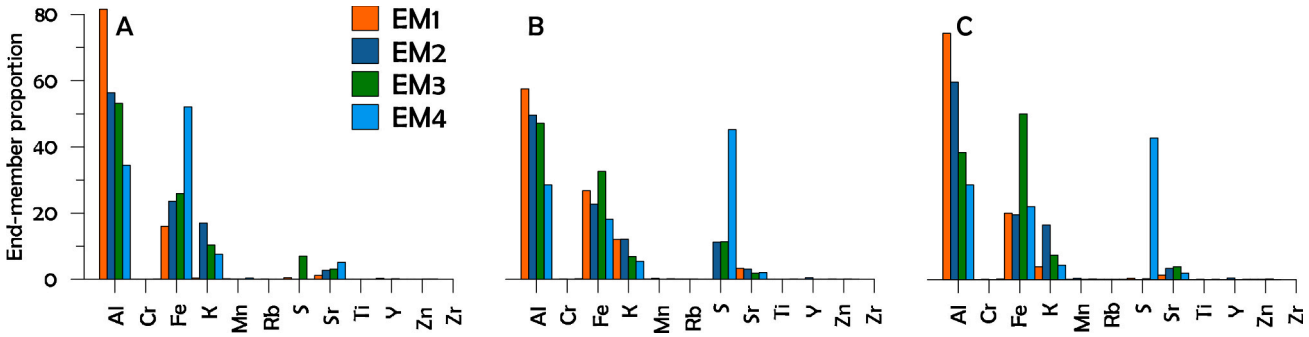

Fig. 4. End-member models based on the chemical data set of N = 12 elements, calculated separately for the PSA samples, (A), the core (B) and the combined data set (C).

Methods

PSA samples

The collection of the clay fraction of samples taken in the Murray Darling Basin (Fig. 1) is already fully documented in Gingele and De Deckker (2005) as well for geochemical analytical procedures using wavelength-dispersive XRF on fused beads on these samples. The original river samples were collected adjacent to rivers, from river banks and high flood levels from bridge pylons, and similar features that had been deposited during major flood events. Overbank samples represent the average composition of the river catchment, although they can also become a source of aeolian sediments during periods of drought, but in general these are considered of less importance with respect to the amount of fluvial sediments originating from the MDB.

The same procedure was followed for samples collected from central and western South Australia; this time, the samples were obtained from potential source areas [PSA] of dust deflation, many of which were on the sides of large saline playas. For more information, consult De Deckker (2019) and De Deckker (2020). All samples, from all PSAs, were eventually (re-)measured by XRF-CS and calibrated using Inductively Coupled Plasma Mass Spectrometry (ICP-MS) measurements through a multivariate log-ratio calibration (MLC) approach (Weltje et al., 2015), resulting in quantitative data (ppm).

Core MD03-2607

Core MD03-2607 was recovered from the South Australian continental slope at 36° 57.640′S / 137° 24.390′E and a water depth of 865 m. Straight after the core was obtained at sea, it was split lengthwise and described (see Hill and De Deckker, 2003). In addition, colour reflectance of the entire core was obtained following the technique applied by

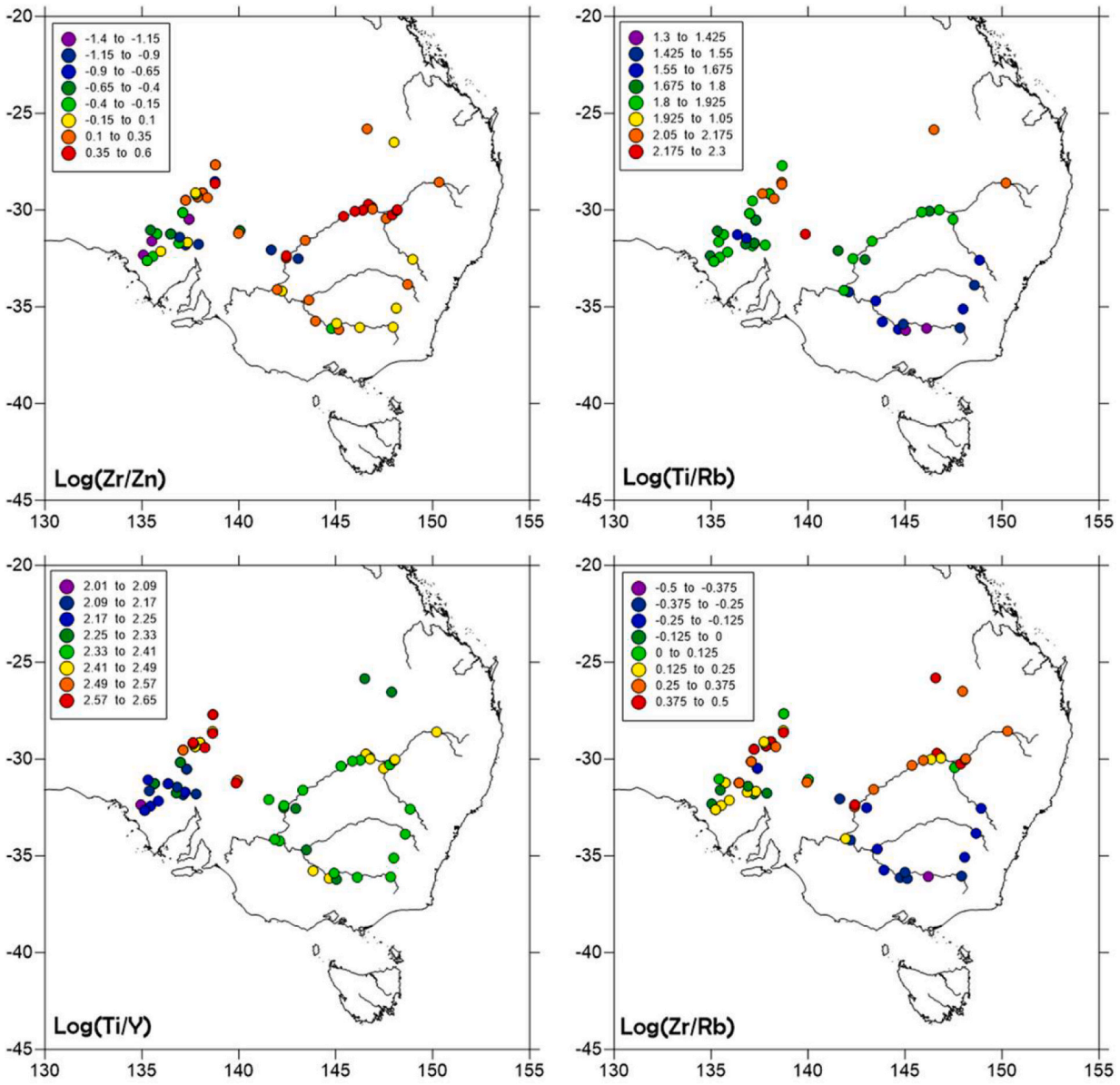

Fig. 5. Spatial distribution of element ratios showing the characteristic differences of the PSAs. In this figure, the colour scale is defined by the amplitude in values of the respective elemental ratios.

Lourens (2004) to deep-sea cores in the Mediterranean Sea. The measurements were carried out while at sea soon after the opening of the core. A Minolta CM-508 spectrophotometer was used. Measurements were made every cm for the upper 10.5 m of the core and below that (until 32.95 m) this was done at 2 cm intervals. The various colour reflectance signals (see: De Deckker et al., 2021) appear to parallel the $\delta^{18}O$ curve of planktic foraminifera, as well as a sea-surface temperature curve already obtained by Lopes dos Santos et al. (2013) and supplemented by De Deckker et al. (2019). We can therefore assume with confidence that the core has not been affected by hiatuses nor reworking.

A 2 cm x 2 cm u-channel was taken from the entire core MD03-2607 and the bulk elemental composition (*in situ* viz. in the core and therefore with no pre-treatment applied) was obtained following the procedure presented in Stuut et al. (2014) using an AvaaTech XRF core scanner at 1-cm resolution at the Royal Netherlands Institute for Sea Research (NIOZ) (Richter et al., 2006). For more information on the core and its location, refer to Fig. 1 and De Deckker et al. (2021). In order to make the data of the core comparable to that of the PSA samples, we also calibrated this XRF-CS record using the MLC approach (Weltje et al., 2015) with (N = 24) calibration samples from the core and measured through ICP-MS.

There have already been a number of published studies carried out on core MD03-2607 for which we now have an outstanding chronology, not only based on the $\delta^{18}O$ of planktic foraminifera, but also on 24 AMS radiocarbon dates obtained from planktic foraminifera and also 16 OSL dates. In addition, 16 tie points (plus 2 outliers probably as a result of micro-turbidites) for the lower portion of the core down to 13.6 m were obtained by comparing the $\delta^{18}O$ of benthic foraminifera from the core and compared with the $\delta^{18}O$ stack record of core MD97-2120 taken offshore New Zealand (Lisiecki and Stern, 2016) and that is bathed by Intermediate Waters from the Pacific Ocean since it was taken at a similar water depth as core MD03-2607. The chronology was modelled using the Bayesian OxCal P sequence (deposition sequence) with variable deposition rate that is presented in De Deckker et al. (2021). In addition, a detailed analysis of the pollen content of core MD03-2607 was performed by Sander van der Kaars in De Deckker et al., (2021), followed by the analysis of pollen and spore taxa before and after the

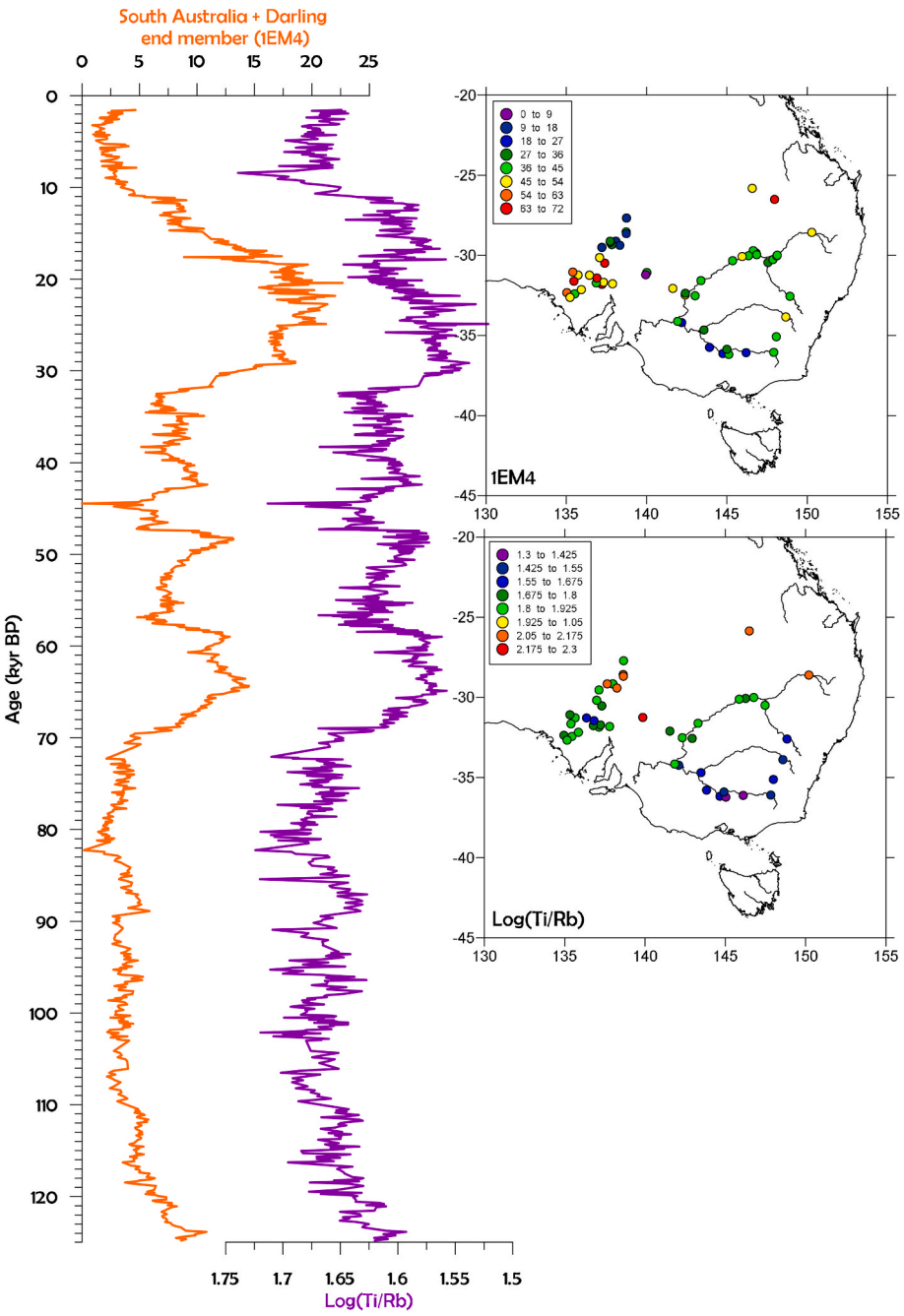

Fig. 6. Proxies for Darling River and central and western South Australia, reconstructed for core MD03-2607. Relative downcore contribution of the first end member of the four end-member model, which is compared with the downcore Log(Ti/Rb) ratio, covering the last 125 kyrs. Also shown are the spatial distributions of the first of the four end-member model and the spatial distribution of the element log-ratio Ti/Rb, which show clear differences between the PSAs.

timing of the megafaunal extinction in the MDB. These studies followed on from the investigations of Lopes dos Santos et al. (2013a,b) who not only looked at the composition of the planktic foraminifer populations in the same core, but also assessed the organic compounds in the core to determine past sea-surface temperatures (using $U^{K'}_{37}$, TEX^{H}_{86}, and LDI) as well as the biomarker of megafires called Levoglucosan). These studies also relied on foraminifer isotope stratigraphy. Finally, Bayon et al. (2017) examined Nd isotopes in that core to determine changes in sediment provenance in the MDB through time.

End-member modelling

Instead of comparing individual element ratios to characterise PSAs, we followed an end-member approach, which assumes that compositional data can be "unmixed" into end members. This approach has been successfully applied to datasets of particle-size distributions. In the case of particle sizes, the end members are interpreted as being the result of sediment-transport mechanisms. In our case of compositional data of bulk chemical data, we test the hypothesis that core samples are mixtures of sediments originating from a limited amount of PSAs. End members were calculated using the program Analysize (Paterson and Heslop, 2015), which was shown to be the most objective algorithm to deconvolve (particle-size) distributions (Van Hateren et al., 2018), but which can be applied to unmix any compositional dataset. The approach is based on a numerical model that attempts to unmix any given dataset of compositional data without any *a priori* information. For example, in

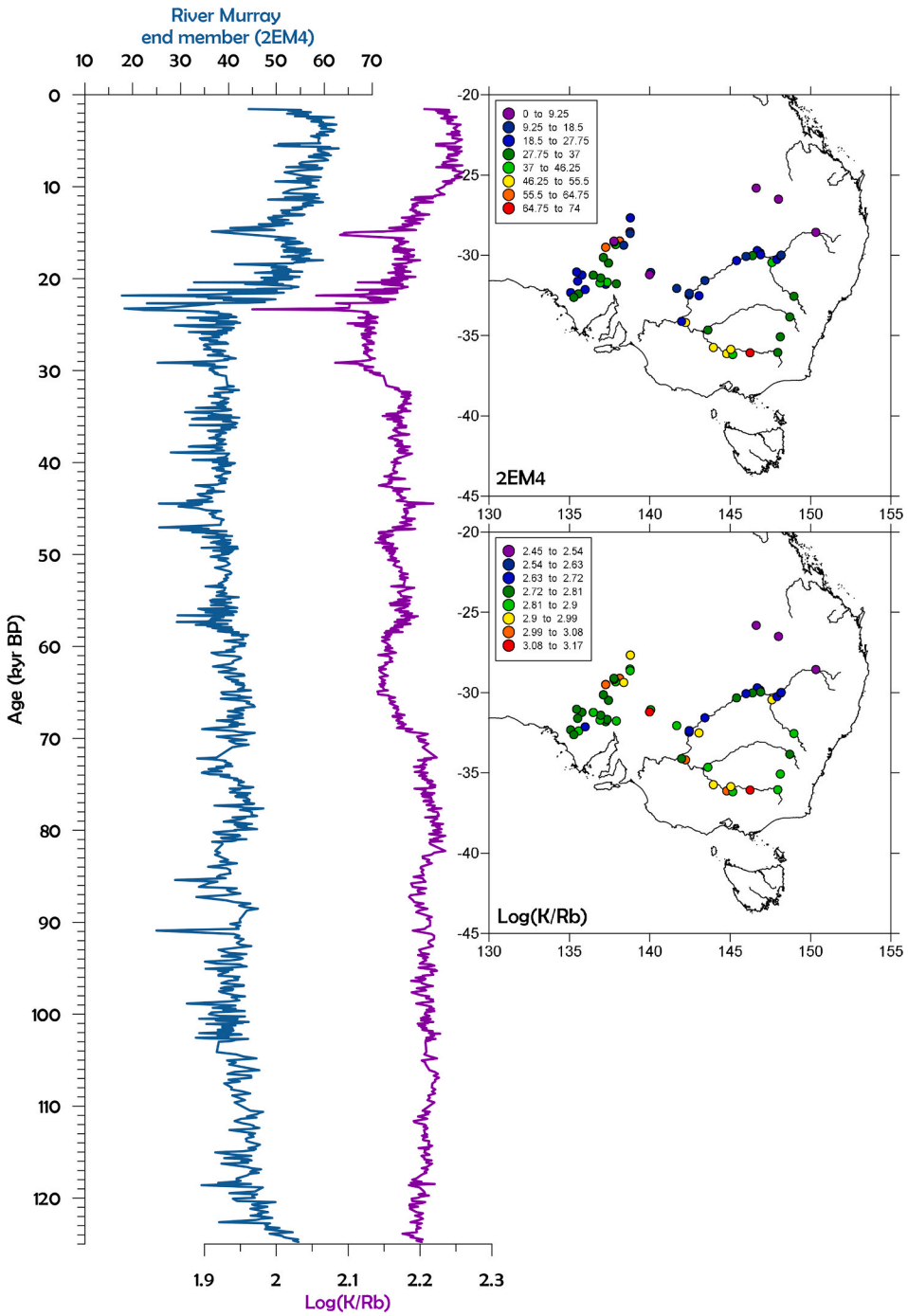

Fig. 7. Proxies for River Murray, reconstructed for core MD03-2607. Relative downcore contribution of the second of the four end-member model, which is compared with the downcore Log(K/Rb) ratio, covering the last 125 kyrs. Also shown are the spatial distributions of the second of the four end-member model and the spatial distribution of the element log-ratio K/Rb, which show clear differences between the PSAs.

the case of particle-size distributions, no assumptions are made about the shape of the particle-size distribution of the modelled end members. The number of end members to be used for a satisfactory description of the variability in the data set is based on the goodness-of-fit statistics (Weltje, 1997). To be able to determine the end members, the element data had to be expressed as percentages, potentially leading to an overestimation of the contribution of abundant elements like aluminium (Al), silicium (Si), sulphur (S), potassium (K), calcium (Ca), iron (Fe), and strontium (Sr). In contrast, elements with much lower abundances like titanium (Ti), manganese (Mn), rubidium (Rb), yttrium (Y) and zircon (Zr) will be underrepresented in this modelling approach. Finally, not all elements were measured for all samples, or could be quantified by the regression based on ICP-MS analyses. As a result, the selection of elements used in the comparison was limited to N = 12: Al, S, K, Ti, Cr, Mn, Fe, Zn, Rb, Sr, Y, and Zr.

End-member compositions were calculated separately for the sediment core (N = 1164 samples) and the source sediments (N = 72), resulting in end-member models with up to N = 10 end members. The amount of end members was determined based on the goodness-of-fit statistics (Fig. 2) as well as their downcore abundance in core MD03-2607 and their spatial distribution. The results of the three-, four- and five end-member models are shown in the supplementary material.

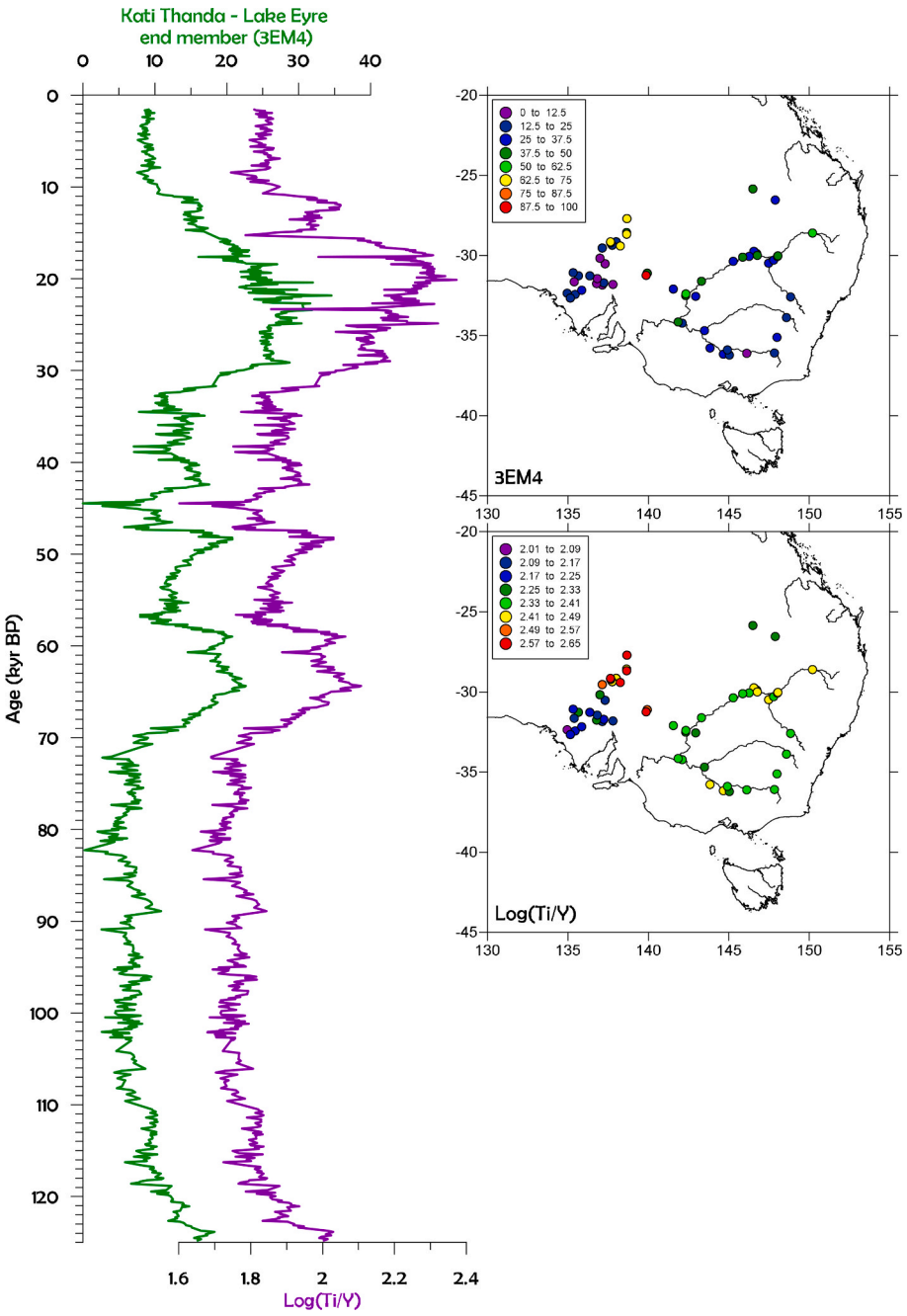

Fig. 8. Proxies for the Kati Thanda – Lake Eyre region, reconstructed for core MD03-2607. Relative downcore contribution of the third of the four end-member model, which is compared with the downcore Log(Ti/Y) ratio, covering the last 125 kyrs. Also shown are the spatial distributions of the third end member of the four end-member model and the spatial distribution of the element log-ratio Ti/Y, which show clear differences between the PSAs.

Results

Fingerprinting of three modern-day regions of southeastern Australia

The dataset of N = 72 surface samples collected from the different PSAs was initially analysed using particular element ratios. To demonstrate that on the basis of bulk chemistry different regions can be characterized with different element ratios, Fig. 3 shows plots of the elements Rb versus Zr and Ti versus Y. Based on this approach, we can make a distinction between Kati Thanda – Lake Eyre and the region of South Australia. However, these elements were present only in relatively low amounts in both the PSA samples as well as the sediment core, and hence they did not play a large role in the end-member calculations. It is clear that the spread in the PSAs of dust is much larger than the spread in the MDB River catchments.

End-member modelling of bulk-chemical data

Fig. 4 shows the distribution of end members calculated separately for the PSA samples (Fig. 4A), for the sediment core MD03-2607 (Fig. 4B) and for the combined data set of core and PSAs for four end members (Fig. 4C). Only a few elements of the N = 12 that were used in the modelling, to determine the composition of the end members. The distribution of the elements across the four end members is very comparable between the three different end-member models.

Next to the modelled chemical data, a number of additional

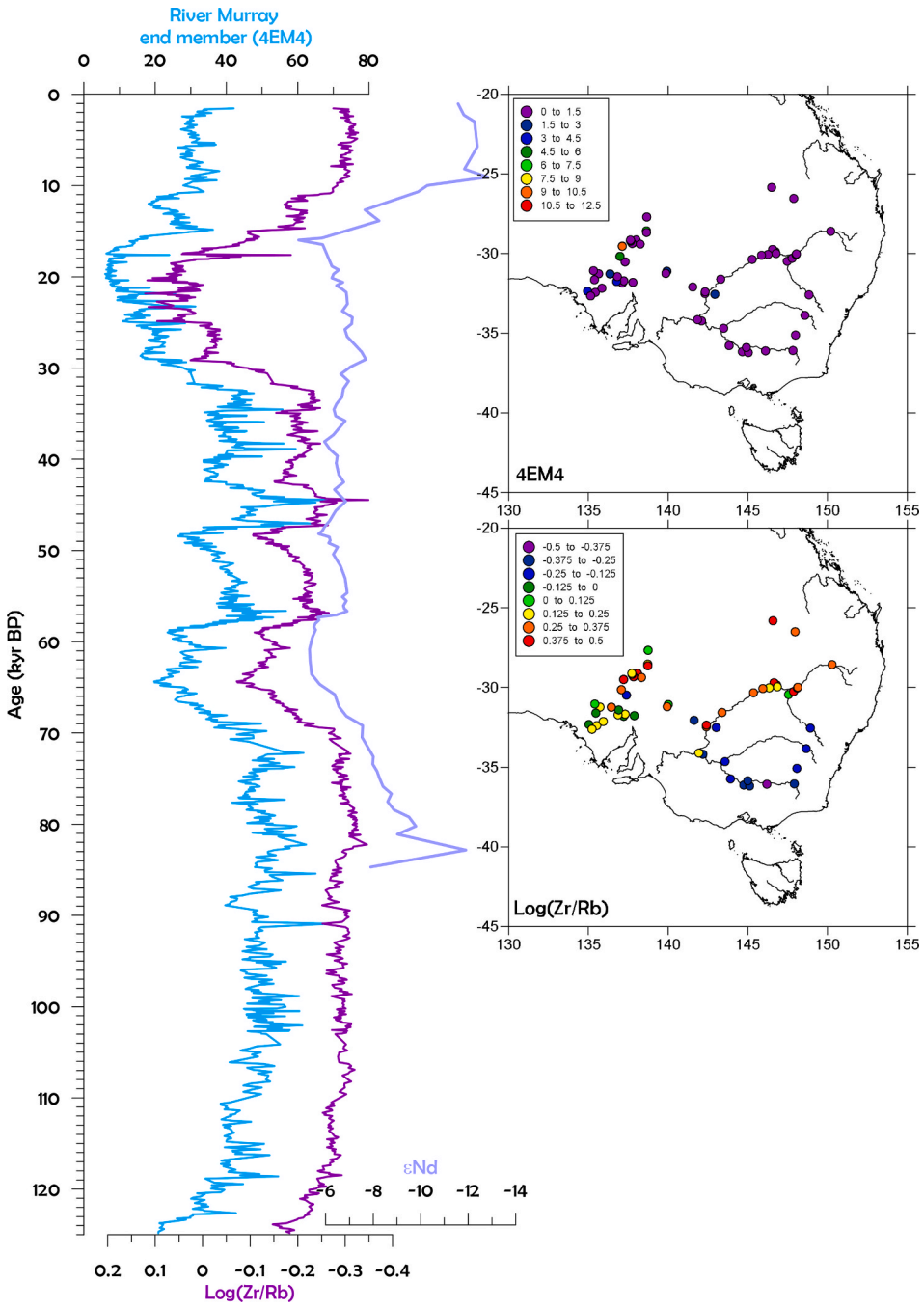

Fig. 9. Proxies for River Murray, reconstructed for core MD03-2607. Relative downcore contribution of the fourth of the four end-member model, which is compared with the downcore Log(Zr/Rb) ratio, covering the last 125 kyrs, as well as the eNd measured on the same core (Bayon et al., 2017), covering the last 85 kyrs that shows a value around −6 attributed to Darling River (and tributaries) sediments, and Holocene values (and ~ 84 kyrs) attributed to the River Murray and tributaries. Also shown are the spatial distributions of the fourth of the four end-member model and the spatial distribution of the element log-ratio Zr/Rb, showing clear differences between the PSAs.

elemental ratios were selected that provide support for the end-member interpretations of the single-element end members such as Zr/Zn, Ti/Rb, Ti/Y and Zr/Rb (Fig. 6).

In addition to the spatial distribution of the end members, their downcore occurrence in sediment core MD03-2607 can be interpreted as the relative contribution downcore of each of the PSAs through time (Figs. 6-9). Comparison with published provenance data (e.g., εNd, clay-mineral content, XRF core-scan data from the thorough review of De Deckker et al., 2021) were also taken into account for the interpretation of the end members in terms of provenance and sediment-transport mechanism.

Discussion

Provenancing the terrigenous sediments in core MD03-2607

Since the core is located offshore the mouth of the River Murray, it is obvious that much of the terrigenous sediments originate from the MDB. Typically, the river-derived sediment fraction found in deep-marine sediment cores is very fine-grained (e.g. Prins et al., 2000; Stuut et al., 2002; Mulitza et al., 2010). Yet, in our study we are comparing the clay-sized fraction of land samples with the bulk (no size separation) fraction of the sediments in the core. To verify if this approach is valid, we took

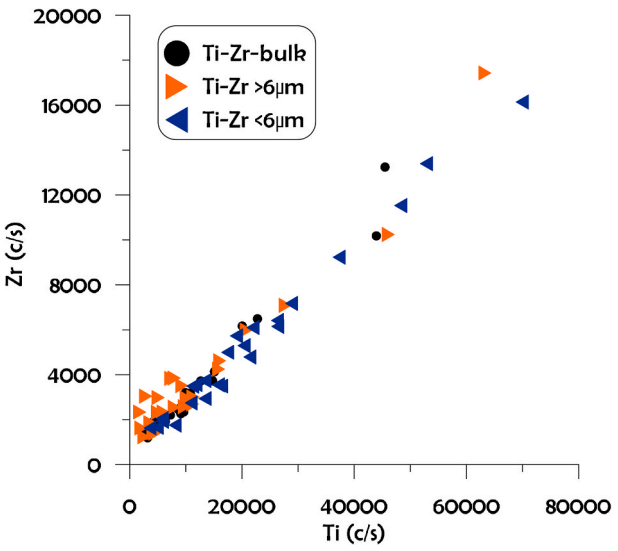

Fig. 10. Comparison of N = 25 samples taken randomly from core MD03-2607 and split into two size fractions, larger and smaller than 6 µm, based on settling techniques. Of three size fractions (bulk, >6µm and < 6 µm) the ratio of Ti and Zr is plotted, demonstrating that there is hardly any difference between the different size fractions and their chemical composition.

N = 25 randomly distributed samples from core MD03-2607 and size-separated them at 6 µm, using the same settling-based technique as Gingele and De Deckker (2005). Consequently, we analysed their bulk and size separated chemical compositions with the same XRF scanning method. Fig. 10 shows the result for the elements Ti and Zr, demonstrating that indeed there is no significant difference in chemical composition between the three fractions: bulk, <6µm and > 6 µm.

Despite the fact that most material in the core is derived from the MDB, we show that it is possible to attribute material from the two geochemically-distinct sub-basins as was already done for clay compositions and Sr and Nd isotopic ratios (Gingele and De Deckker, 2005). However, as XRF-CS data are acquired here at a very high resolution of every cm down core, this approach can provide much more information than for the data acquired by sporadic sampling for clays and isotopes as done by Gingele and De Deckker (2004; 2005). In addition, it is now clear that some trace elemental ratios of sediments recovered in the core do not relate to the MDB but instead from another source(s), viz. central and western South Australia. The sediments from such sources must have instead been airborne as there are no significant rivers to drain these regions to the sea (refer to the maps in De Deckker, 2021).

The new approach we are taking here is to numerically decompose the mixture of bulk chemical compositions of on-land samples and a sediment core that consists of the relative contributions of the PSAs by rivers and by wind.

The selection of the elements used in the comparison was limited to 12 elements: Al, S, K, Ti, Cr, Mn, Fe, Zn, Rb, Sr, Y, and Zr. The consequent end members that were calculated by the models turned out to consist of yet another smaller selection of mainly seven elements (Al, S, K, Fe, Mn, Rb, Sr) that enabled us to satisfactorily describe the variability in the data set. However, the other elements, that were not used in the modelling turned out to be characteristic for the different PSAs as well, and could be used as log-ratios (Zr/Zn, Ti/Rb, Ti/Y and Zr/Rb) to distinguish the PSAs from one another (see Fig. 5). Finally, the log-ratios also compensate for eventual unevenness's in the core U-channels (Weltje and Tjallingii, 2008).

The combination of spatial distributions of end-member occurrences and Log-ratio values of the different elements was then used to define three different PSAs: Darling River, Kati Thanda – Lake Eyre and south and central South Australia, and River Murray. This eventually Thanda – Lake Eyre, and enabled us to determine the various contributions of each PSA in core MD03-2607 throughout the past 125 kyrs. These are presented in a chronological order in the following section. It is worth remembering that the sediments from the Kati Thanda – Lake Eyre District and south and central South Australia, can only be transported to the core by wind as this basin is endorheic.

Late Quaternary paleo-environmental history registered by sediment core MD03-2607

Before considering the history of deposition of sediments at the core site, it is necessary to consider that sea level through the last glacial-interglacial cycle fluctuated by about 125 m (Yokoyama et al., 2022). This means that the mouth of the River Murray, that is today located some 200 km from the core site, was only 15 km away from the core site during the Last Glacial Maximum. However, one ought to consider that the exposed Lacepede Shelf (Fig. 1) during periods of low sea level would have contributed some sediments vias aeolian processes. We know that that shelf consisted much of quartz dunes (see Nash et al., 2018).

As a result, the colour of the sediments in the core-reflectance profile (Michel, 2003; De Deckker et al., 2021, their supplement Fig. 5) shows darker tints during periods of low sea-level, and paler colours during sea-level high stands. The latter is due to the greater supply of pelagic muds (consisting mostly of planktonic foraminifera and coccolithophores) whereas an increase of terrigenous organic matter would have been transported at sea by the River Murray through its mouth.

The environmental history recorded at the core site is interpreted below and can be visualized through examination of Fig. 11. River Murray sediments are represented by two end members, light blue and dark blue in Fig. 11. It appears that end member 2, interpreted as representing River Murray sediments, fluctuates very little throughout the record, except for the last 14 kyr, when it significantly increased and predominates among the four end members.

1. During MIS5e, the contribution of Darling River sediments declined from 8 to 4 % and this is matched by a progressive increase of River Murray sediments.
2. From the end of MIS5e until the onset of MIS4 (the remainder of MIS5, comprising 5d-5a) there was very little sediment fluctuation. The contribution of Kati Thanda – Lake Eyre sediments was minimal, whereas the predominant supply came from the River Murray as also shown by the low values (~-12, see Fig. 10) for the Nd isotopes shown by Bayon et al., (2017).
3. During MIS4, when sea level was very low (−80.7 ± 6 m; based on Grant et al., 2012) and glacial conditions occurred, the supply of Kati Thanda – Lake Eyre sediments increased significantly (shown by the green curve in Fig. 11) peaking twice at 65 kyr BP and at 59 kyr BP. Even as the core site was much closer to the Australian shoreline, there does not appear to be a significant increase in the sedimentation rates at the core site. This is also matched by an increase of sediment originating from the Darling River catchment (Fig. 11). This could imply varying wind directions.
4. After termination of MIS4, there was a significant decrease in Darling River sediments and very strong fluctuations in River Murray sediments. There were two episodes of minimal contribution of Kati Thanda – Lake Eyre region sediments at 47 and 45 kyr BP, respectively. These episodes were rather short. The polar front was closer to southern Australia at those times and the Australian continent was known to be very cold as recognised by De Deckker et al. (2020; their Fig. 2) using the presence of planktonic foraminifera in core MD03-2611, located some 60 km northwest of core MD03-2607 (see De Deckker et al., 2020; their Fig. 1). However, the reconstructed alkenone sea-surface temperatures from core MD03-2607 only showed minor fluctuations (see De Deckker et al., 2020; their Fig. 2B).

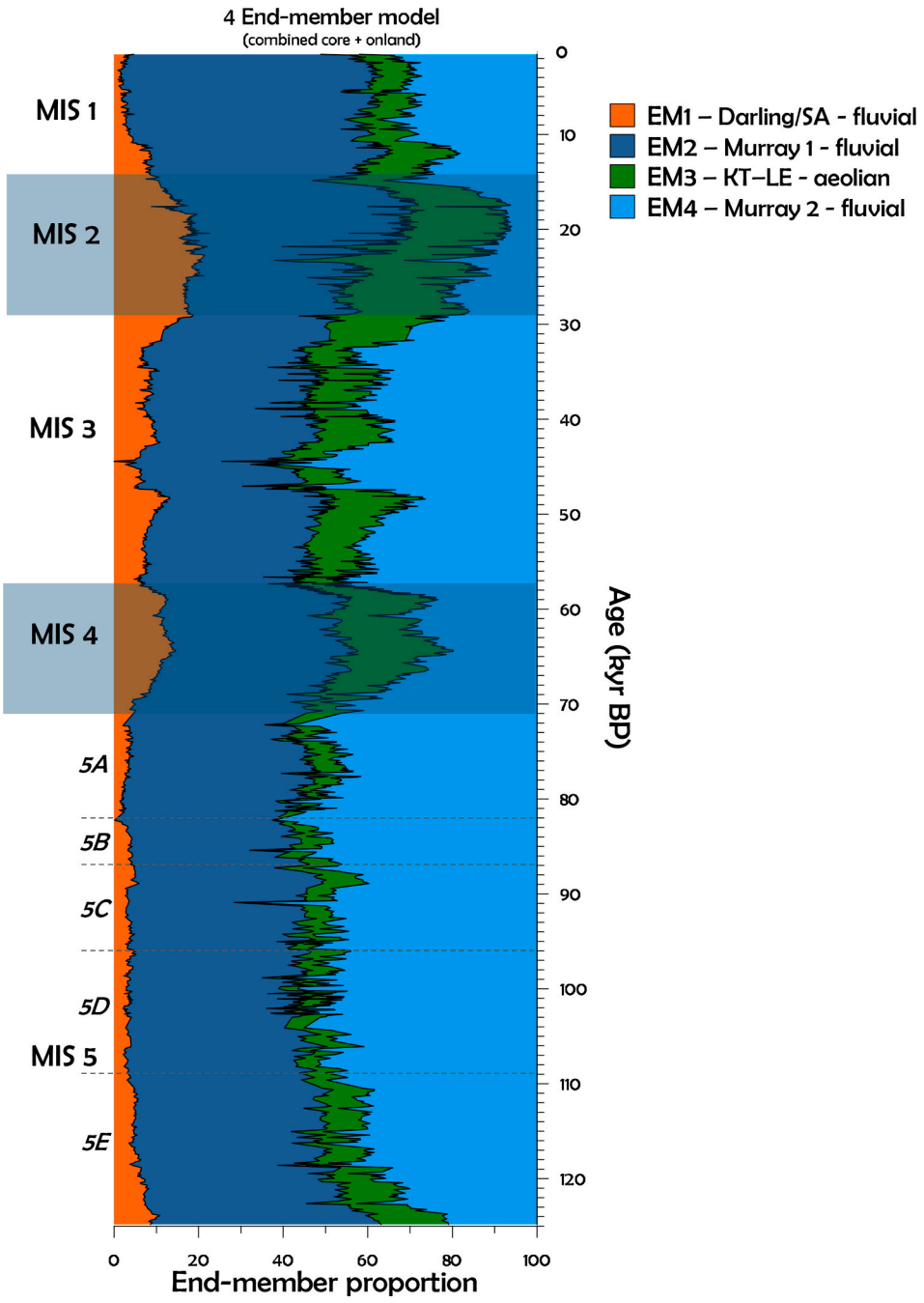

Fig. 11. Downcore proportion of each of the four end members calculated in the four-end-member model in core MD03-2607 for the last 125 kyr. Glacial- and interglacial stages are indicated; dark horizontal bands indicate glacials MIS4 and MIS2.

5. From 33 kyr BP, there was a progressive change with significant increase of end member 3 (Kati Thanda – Lake Eyre), with a sudden increase at 28 kyr BP, and which culminates at the LGM (24 – 18 kyr BP). This implies a significant supply of aeolian sediments from that region.
6. Between 21 and 18 kyr BP, the contribution of end member 3 that continued after the LGM, to eventually progressively decrease down to 15 kyr BP. This is seen in Fig. 11 for both end members 1 (orange) and 3 (green). This observation is corroborated by Cosentino et al., 2024 who calculated a threefold increase in dust deposited between 26 and 19 kyr BP.
7. From 14.5 to 13 kyr BP, there was again an increase of end member 3, which is likely to correspond to the Antarctic Cold Reversal (ACR; Pedro et al., 2016).
8. Already from after the LGM end member 2, representing the River Murray sediment component progressively increasing, apart from the little ACR episode. This contrasts with the percentage of that end member (2EM4, dark blue in Fig. 11) during MIS5e. We note, however, that the Murray River component gently decreased from the latter part of the Holocene (3 kyr BP) to the top of the core.
9. The Nd isotopes measurements made by Bayon et al. (2017) further support the interpretations on the XRF data presented herewith.

We need to consider, as documented by modern-day dust distribution in southeastern Australia, that when the Westerlies move across southeastern Australia, any dust plume would travel perpendicularly to the movement of the arcuate fronts (De Deckker et al., 2008). In other words, if a front moves across central and western South Australia, it is

more than plausible that a dust plume originating from that area would reach the core site. Consequently, during the glacials, the path of the Westerlies was displaced towards the North, thereby increasing the area from which dust could be emitted, transported and eventually deposited at sea. As a result, during the glacial phases, Westerlies would have been travelling over a large part of southern Australia.

Conclusions

Together with a good set of trace-elemental analyses gathered on land, it has been possible to ascertain the origin of the terrigenous sediment in a deep-sea core. Naturally, knowledge of the local drainage of a land mass to the ocean can also help determine if the sediments are fluvially transported or airborne. In addition, the critical choice of elements and their ratios can help identify the sediments origin, such as is the case for the three regions considered here. In this case, the Zr/Rb and Ti/Y have proven to be suitable ratios. Finally, we are also able to determine atmospheric conditions that led to the delivery of sediments to the core site.

CRediT authorship contribution statement

Jan-Berend W. Stuut: Writing – review & editing, Writing – original draft, Formal analysis, Conceptualization, Methodology. **Patrick De Deckker:** Writing – review & editing, Writing – original draft, Resources. **Rick Hennekam:** Writing – review & editing, Methodology.

Declaration of competing interest

The authors declare that they have no known competing financial interests or personal relationships that could have influenced the work reported in this paper.

Acknowledgements

We greatly acknowledge the late Rineke Gieles for her substantial help with the XRF scanning of the core. This work was financed by NIOZ and Australian ARC discovery grant DP0772180. We are very grateful for the pertinent comments of the three anonymous reviewers that helped improve the quality and readability of the manuscript. Thank you to them all.

Appendix A. Supplementary data

Supplementary data to this article can be found online at https://doi.org/10.1016/j.aeolia.2025.100997.

Data availability

All data are in the process of being stored in the open-access database www.pangaea.de.

References

Bayon, G., De Deckker, P., Magee, J.W., Germain, Y., Bermell, S., Tachikawa, K., Norman, M.D., 2017. Extensive wet episodes in late Glacial Australia resulting from high-latitude forcings. Sci. Rep. 7, 44054.

Boyle, E.A., 1983. Chemical accumulation variations under the Peru current during the past 130,000 years. J. Geophys. Res. 88, 7667–7680.

Cosentino, N.J., Torre, G., Lambert, F., Albani, S., De Vleeschouwer, F., Bory, A.J.M., 2024. Paleo±Dust: quantifying uncertainty in paleo-dust deposition across archive types. Earth Syst. Sci. Data 16, 941–959.

De Deckker, P., 2019. An evaluation of Australia as a major source of dust. Earth Sci. Rev. 194, 536–567.

De Deckker, P., 2020. Airborne dust traffic from Australia in modern and Late Quaternary times. Global Planet. Change 184, 103056, 19 pp.

De Deckker, P., Arnold, L.J., van der Kaars, S., Bayon, G., Stuut, J.-B.-W., Perner, K., Lopes dos Santos, R., Uemura, R., Demuro, M., 2019. Marine Isotope Stage 4 in Australasia: a full glacial culminating 65,000 years ago – global connections and implications for human dispersal. Quat. Sci. Rev. 204, 187–207.

De Deckker, P., Haberle, S., van der Kaars, S., Hua, Q., Stuut, J.-B.-W., 2021. The pollen record of marine core MD03-2607 offshore Kangaroo Island spanning the last 125 kyears; implications for vegetation changes across the Murray-Darling Basin. Aust. J. Earth Sci. 68. https://doi.org/10.1080/08120099.2021.1896578.

De Deckker, P., Munday, C., Brocks, J., O'loinsigh, T., Alison, G., Hope, J., Norman, M., Stuut, J.-B., Tapper, N.J., Van der Kaars, S., 2014. Characterisation of the major dust storm that traversed over eastern Australia in September 2009; a multidisciplinary approach. Aeolian Research 15, 133-149.

Gingele, F.X., De Deckker, P., 2005. Clay mineral, geochemical and Sr-Nd-isotopic fingerprinting of sediments in the Murray-Darling fluvial system, SE Australia. Australian Journal of Earth Science 52, 965–974.

Gingele, F.X., De Deckker, P., Hillenbrand, C.-D., 2004. Late Quaternary terrigenous sediments from the Murray Canyons area, offshore South Australia and their implications for sea level change, palaeoclimate and palaeodrainage of the Murray-Darling Basin. Mar. Geol. 212, 183–197.

Gingele, F.X., De Deckker, P., Norman, M., 2007. Late Pleistocene and Holocene climate of SE Australia reconstructed from dust and river loads deposited offshore the River Murray Mouth. Earth Planet. Sci. Lett. 255, 257–272.

Grant, K., Rohling, E., Bar-Matthews, M., Ayalon, A., Medina-Elizalde, M., Bronk Ramsey, C., Satow, C., Roberts, A.P., 2012. Rapid coupling between ice volume and polar temperature over the past 150,000 years. Nature 491, 744–747. https://doi.org/10.1038/nature11593.

Haug, G.H., Hughen, K.A., Sigman, D.M., Peterson, L.C., Röhl, U., 2001. Southward migration of the Intertropical Convergence Zone through the Holocene. Science 293, 1304–1308.

Hill, P., De Deckker, P., 2004. AUSCAN Seafloor Mapping and Geological Sampling Survey on the Australian Southern Margin by RV Marion Dufresne in 2003. Geoscience Australia Record 2004/04, 136pp.

Lamy, F., Hebbeln, D., Röhl, U., Wefer, G., 2001. Holocene rainfall variability in southern Chile: a marine record of latitudinal shifts of the Southern Westerlies. Earth Planet. Sci. Lett. 185, 369–382.

Lamy, F., Gersonde, R., Winckler, G., Esper, O., Jaeschke, A., Kuhn, G., Ullermann, J., Martinez-Garcia, A., Lambert, F., Kilian, R., 2014. Increased Dust Deposition in the Pacific Southern Ocean during Glacial periods. Science 343, 403–407.

Lisiecki, L.E., Stern, J.V., 2016. Regional and global benthic δ18O stacks for the last glacial cycle. Paleoceanography 31, 1368–1394. https://doi.org/10.1002/2016PA003002.

Lopes dos Santos, R., Spooner, M.I., Barrows, T.T., De Deckker, P., Sinninghe, J.S., Schouten, S., 2013. Comparison of organic (UK'37, TEXH86, LDI) and faunal proxies (foraminiferal assemblages) for reconstruction of late Quaternary sea surface temperature variability from offshore southeastern Australia. Paleoceanography 28, 1–11. https://doi.org/10.1002/palo.20035.

Lopes Dos Santos, R.A., De Deckker, P., Hopmans, E.C., Magee, J.W., Mets, A., Sinninghe Damsté, J.S., Schouten, S., 2013. Abrupt vegetation change after the Late Quaternary megafaunal extinction in southeastern Australia. Nat. Geosci. https://doi.org/10.1038/NGEO1856.

Lourens, L.J., 2004. Revised tuning of Ocean Drilling Program Site 964 and KC01B (Mediterranean) and implications for the $\delta^{18}O$, tephra, calcareous nannofossil, and geomagnetic reversal chronologies of the past 1.1 Myr. Paleoceanography 19, PA3010. https://doi.org/10.1029/2003PA000997.

McGregor, H.V., Dupont, L., Stuut, J.-B.-W., Kuhlmann, H., 2009. Vegetation change, goats, and religion: a 2000-year history of land use in southern Morocco. Quat. Sci. Rev. 28, 1434–1448.

Matthewson, A.P., Shimmield, G.B., Kroon, D., 1995. A 300 kyr high-resolution aridity record of the North-african continent. Paleoceanography 10, 677–692.

Nash, G., De Deckker, P., Mitchell, C., Murray-Wallace, C.V., Hua, Q., 2018. Micropalaeontological evidence for deglacial marine flooding of the ancient courses of the River Murray across the Lacepede Shelf, southern Australia. Mar. Micropaleontol. 141, 55–72.

Pedro, J.B., Bostock, H.C., Bitz, C.M., He, F., Vandergoes, M.J., Steig, E.J., Chase, B.M., Krause, C.E., Rasmussen, S.O., Markle, B.R., Cortese, G., 2016. The spatial extent and dynamics of the Antarctic Cold Reversal. Nat. Geosci. 9, 51–55.

Prins, M.A., Troelstra, S.R., Kruk, R.W., Borg van der, K., Jong de, A.J., Weltje, G.J., 2001. The Late Quaternary sediment record from Reykjanes Ridge, North Atlantic. Radiocarbon 43, 939–947.

Richter, T.O., van der Gaast, S, Koster, B., Vaars, S., Gieles, R., De Stigter, H.C., De Haas, H., van Weering, T.C.E., 2006. The Avaatech XRF Core Scanner: technical description and applications to NE Atlantic sediments. In: Rothwell, R.G (ed.) New techniques in sediment core analysis. Geological Society of London, Special Publications 267, 39-50.

Sprigg, R.C., 1979. Stranded and submerged sea-beach systems of southeast South Australia and the aeolian cycle. Sed. Geol. 2, 53–96.

Stuut, J.-B., Temmesfeld, F., De Deckker, P., 2014. A 550 kyr record of aeolian activity near North 2014. a 550 ka record of aeolian activity near North West Cape, Australia: inferences from grain-size distributions and bulk chemistry of SE Indian Ocean deep-sea sediments. Quat. Sci. Rev. 83, 83–94.

Stuut, J.-B.-W., De Deckker, P., Saavedra-Pellitero, M., Bassinot, F., Drury, A.J., Walczak, M.H., Nagashima, K., Murayama, M., 2019. A 5.3-Million-Year history of Monsoonal Precipitation in Northwestern Australia. Geophys. Res. Lett. 46, 6946–6954.

Tjallingii, R., Stattegger, K., Wetzel, A., Van Phach, P., 2010. Infilling and flooding of the Mekong River incised valley during deglacial sea-level rise. Quat. Sci. Rev. 29, 1432–1444.

Weltje, G., 1997. End-member modelling of compositional data: Numerical-statistical algorithms for solving the explicit mixing problem. Journal of Mathematical Geology 29, 503–549.
Weltje, G.J., Tjallingii, R., 2008. Calibration of XRF core scanners for quantitative geochemical logging of sediment cores: Theory and application. Earth Planet. Sci. Lett. 274, 423–438.
Weltje, G.J., Bloemsma, M.R., Tjallingii, R., Heslop, D., Röhl, U., Croudace, I.W., 2015. Prediction of Geochemical Composition from XRF Core Scanner Data: a New Multivariate Approach Including Automatic selection of Calibration Samples and Quantification of Uncertainties. Micro-XRF Studies of Sediment Cores 507–534.
Zabel, M., Bickert, T., Dittert, L., Häse, R.R., 1999. Significance of the sedimentary Al:Ti ratio as an indicator for variations in the circulation patterns of the equatorial North Atlantic. Paleoceanography 14, 789–799.
Zabel, M., Schneider, R.R., Wagner, T., Adegbie, A.T., De Vries, U., Kolonic, S., 2001. Late Quaternary climate changes in Central Africa as inferred from terrigenous input to the Niger Fan. Quat. Res. 56, 207–217.